

A NEW CONVECTIVE ADJUSTMENT SCHEME

Alan K. Betts
Visiting Scientist
European Centre for Medium Range Weather Forecasts

OBSERVATIONAL AND THEORETICAL BASIS

Cumulus parameterization started with simple attempts to represent the subgrid-scale effects of convective clouds. Manabe et al. (1965) proposed adjustment toward a moist adiabatic structure in the presence of conditional instability, and Ruo (1965, 1974) proposed a simple cloud model to redistribute the heating and moistening effects of precipitating clouds in the presence of grid scale moisture convergence. The work of Ooyama (1971), and Arakawa and Schubert (1974) initiated a great deal of research attempting to parameterize cloud ensembles using a cloud spectrum and a simple cloud model (Frank, 1983). One of the key objectives of the GARP Atlantic Tropical Experiment (GATE) (Betts, 1974) was to study organized deep convection in the tropics to test and develop convective parameterizations for numerical models. GATE diagnostic studies have documented the complexity of tropical mesoscale convection (Houze and Betts, 1981) from the importance of mesoscale updrafts and downdrafts as well as convective-scale processes down to the effects of the cloud microphysical processes of forcing, melting, and water loading. One might conclude from these phenomenological studies that cloud models of much greater complexity might be needed to parameterize cumulus convection (Frank, 1983). Little progress has been made in this direction however, because it is clearly impossible to attempt to integrate at each grid point in a global model, a cloudscale model of much realism.

This paper represents a marked divergence in philosophy. The primary objective of the proposed parameterization scheme (Betts and Miller, 1984) is to ensure that the local vertical temperature and moisture structures, which in nature are strongly constrained by convection, be realistic in the large-scale model. The concept of a quasi-equilibrium between the cloud field and the large-scale forcing [introduced by Betts (1973) for shallow convection, and Arakawa and Schubert (1974) for deep clouds] has been well-established, at least on larger space and time scales (Lord, 1982). This means that convective regions have characteristic temperature and moisture structures that can be documented observationally and used as the basis of a convective adjustment procedure. Betts (1973) and Albrecht et al. (1979) modeled shallow convection using this approach. The main limitation of the

moist adiabatic convective adjustment suggested by Manabe et al. (1966) for deep convection is that the tropical atmosphere does not approach a moist adiabatic equilibrium structure in the presence of deep convection. In the scheme proposed here, the temperature and moisture structures will be adjusted simultaneously toward observed quasi-equilibrium structures. This ensures that on the grid scale a global model always maintains a realistic vertical temperature and moisture structure in the presence of convection. This sidesteps all the details of how the subgrid-scale cloud processes maintain the quasi-equilibrium structures one observes. To the extent that one can show observationally that different convective regions have different quasi-equilibrium thermodynamic structures (as a function of wind-field, for example), these could be incorporated using different adjustment parameters. However, in this paper just the simplest scheme to show its usefulness is introduced.

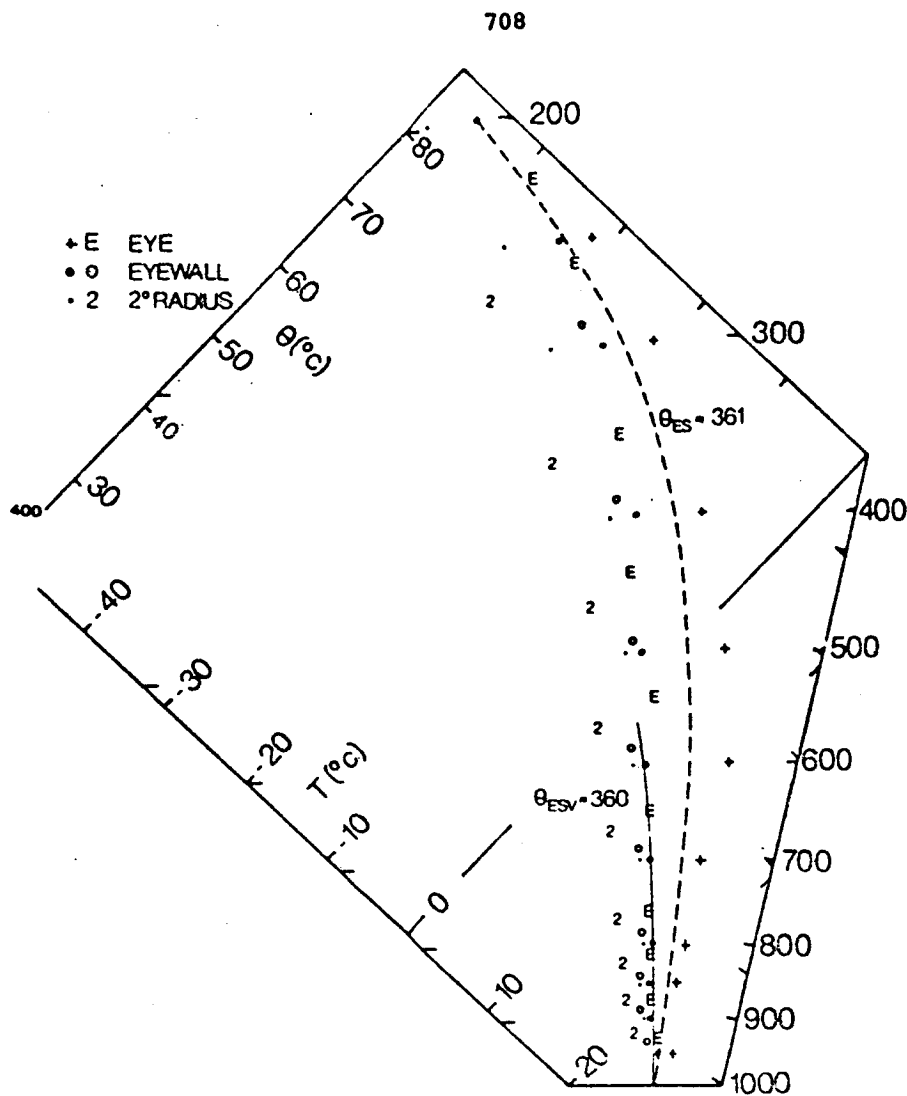
The saturation point formulation of moist thermodynamics (Betts, 1982a) will be used to introduce the observational and theoretical basis of the proposed convective adjustment. The scheme is then applied to a series of data sets from GATE, BOMEX, ATEX and an Arctic air-mass transformation to show the sensitivity of the scheme to different parameters and develop a parameter set suitable for both shallow and deep convection in a global model. The last section (in preparation) will show the effect of the scheme on global forecasts.

Observational Basis

Betts (1982a) has given examples of deep and shallow convective equilibrium structures, and Betts (1983) has discussed equilibrium structure for mixed cumulus layers. Here a few examples are presented that inspired the parameterization scheme. Tephigrams will be presented showing temperature and saturation points ((T, p)) at the lifting condensation level: abbreviated SP). Isopleths of virtual potential temperature (θ_{ESV}) for cloudy air will be shown for reference (Betts, 1983), together with ρ , the pressure departure of air at each pressure level from its saturation level.

Deep Convection: Convective Soundings Over the Tropical Ocean

Figure 1 shows the structure of the deep troposphere for the mean typhoon sounding from Frank (1977). The heavy dots and open circles are temperature and saturation points (T, SP) for the eyewall. They show a temperature structure that parallels a θ_{ESV} isopleth below 600 mb and θ_{ES} increasing above, with a nearly saturated atmosphere ($P_{Si} - p = \rho = -15$ mb). The crosses and symbols E are (T, SP) inside the eyewall. Here the strong subsidence has produced a very stable thermal structure, but the SP structure is very close to the temperature structure of the eyewall: it has been generated by subsidence of air originally saturated at the eyewall temperature (this does not modify the SP). The midtropospheric subsidence within the eye



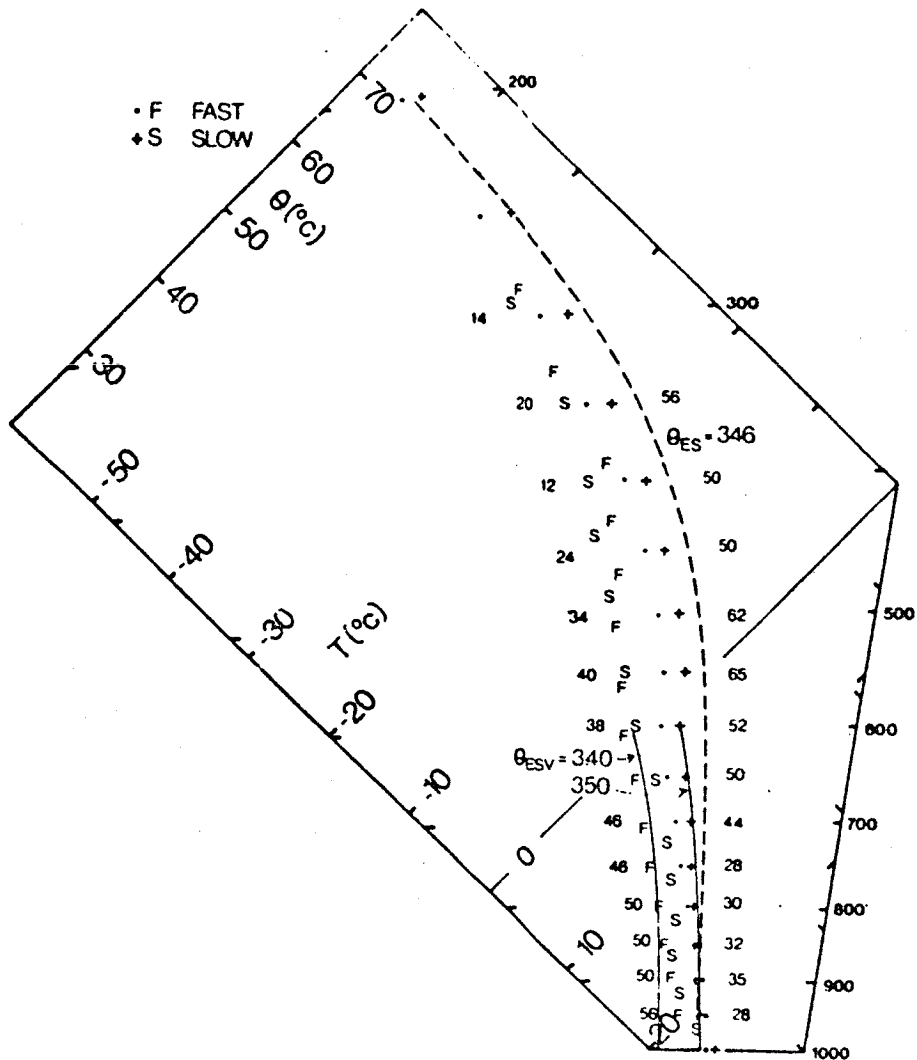


FIGURE 2 Fast and slow moving GATE lines.

is close to the freezing level. The dots and letter F denote the (T, SP) of fast-moving lines (Barnes and Sieckman, 1983), and the cross and letter S denote (T, SP) for slow-moving lines. They show some thermodynamic differences. The ρ values for each p level are shown (fast moving on left, slow on right). For reference, $\rho = 100$ mb corresponds to a relative humidity of 85 percent at 800 mb, 75 percent at 500 mb, and 32 percent at 200 mb at tropical temperatures. The fast-moving line wake has a drier lower troposphere as a result of stronger downdrafts. Its 600 mb temperature is cooler, probably as a response to the falling θ_E in low levels. It is nearly saturated

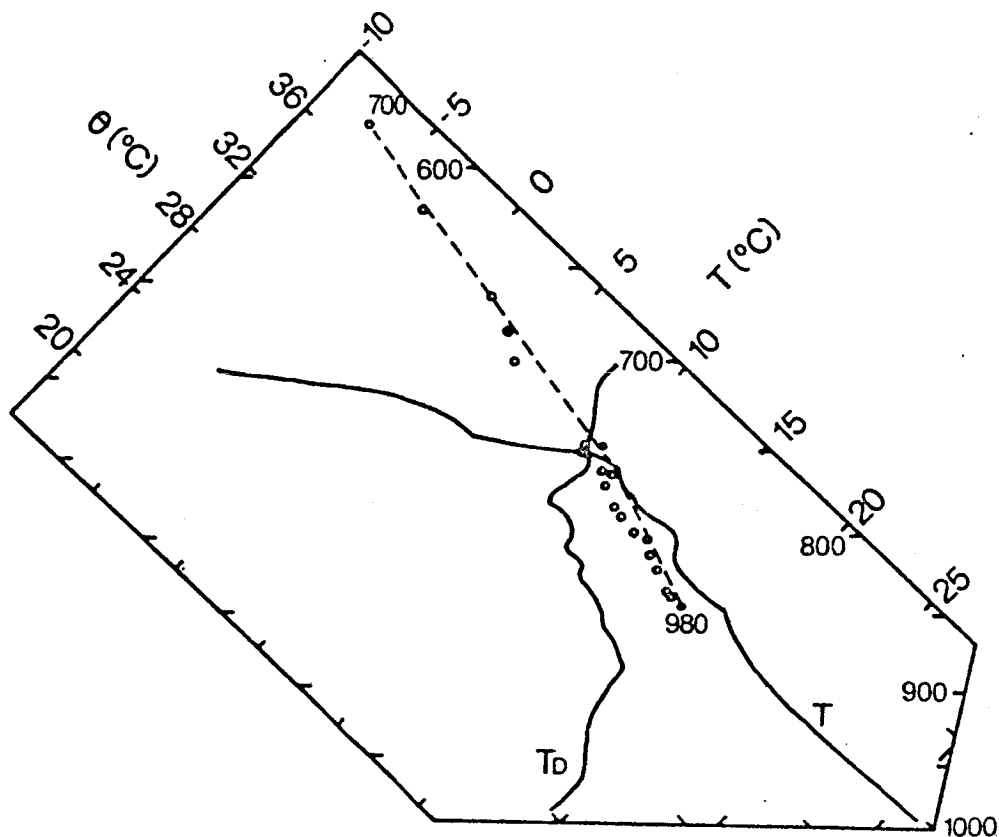


FIGURE 3 Shallow convection mixing line structure.

in the upper troposphere corresponding to extensive anvil clouds. The slow-moving line wake shows the reverse, with a moister lower tropospheric structure and θ_{ES} to 600 mb more closely aligned along a θ_{ESV} isopleth. It however is drier in the upper troposphere. These thermodynamic differences are associated with distinct dynamic features in the wind profile. The fast-moving lines have strong shear between the surface and 650 mb (Barnes and Sieckman, 1984).

Shallow Cumulus Convection: Mixing Line Structure

Cumulus convection is a moist mixing process between the subcloud layer and drier air aloft, and not surprisingly the thermodynamic structure tends toward a mixing line (Betts, 1982a).

Figure 3 shows the (T, T_D) structure (solid lines) and corresponding SPs (open circles) from the surface to 700 mb for a late afternoon convective sounding over land in the tropics. The entire SP structure from 980 mb to 700 mb lies close to the mixing line joining

the end-points. There is a patch of cloud near 750 mb and a dry layer above, but these large fluctuations of T and T_D only appear as SP fluctuations up and down the mixing line. The temperature structure in the cloud layer below the stable layer at 700 mb is nearly parallel to the mixing line.

Convective Adjustment Scheme

The scheme is designed to adjust the atmospheric temperature and moisture structure back toward a reference quasi-equilibrium thermodynamic structure in the presence of large-scale radiative and advective processes. Two different reference thermodynamic structures, which are partly specified and partly internally determined, are used for shallow and deep convection, depending on the height of cloudtop.

Formal Structure

The large-scale thermodynamic tendency equation can be written in terms of $SP(\bar{S})$, using the vector notation suggested in Betts (1983), as

$$\frac{\partial \bar{S}}{\partial t} = -\mathbf{v} \cdot \nabla \bar{S} - \bar{\omega} \frac{\partial \bar{S}}{\partial p} - g \frac{\partial R}{\partial p} - g \frac{\partial F}{\partial p} \quad (1)$$

where R , F are the radiative and convective fluxes (including the precipitation flux). The convective flux divergence is parameterized as

$$-g \frac{\partial F}{\partial p} = \frac{E - \bar{S}}{\tau} \quad (2)$$

where E is the reference quasi-equilibrium thermodynamic structure and τ is an adjustment time representative of the convective time scale.

Simplifying the large-scale forcing to the vertical advection and combining (1) and (2) gives

$$\frac{\partial \bar{S}}{\partial t} = \bar{\omega} \frac{\partial \bar{S}}{\partial p} + (E - \bar{S})/\tau \quad (3)$$

Near quasi-equilibrium $\partial \bar{S} / \partial t \approx 0$ so that

$$(E - \bar{S}) \approx \bar{\omega} \frac{\partial \bar{S}}{\partial p} \tau \quad (4)$$

One finds that values of τ from 1 to 2 hours give good results in the presence of realistic forcing. This means that $E - S$ corresponds to about 1 hour's forcing by the large-scale fields, including radiation. For deep convection, the atmosphere will therefore remain slightly cooler and moister than E . Furthermore, for small τ , the atmosphere

will approach \underline{E} so that one may substitute $\underline{\bar{S}} \approx \underline{E}$ in the vertical advection term, giving

$$(\underline{E} - \underline{\bar{S}}) \approx \omega \tau (\partial \underline{E} / \partial p) \quad (5)$$

from which the convective fluxes can be approximately expressed using (2), as

$$\underline{F} = \int \frac{\underline{E} - \underline{\bar{S}}}{\tau} \frac{dp}{g} \approx \int \left(\omega \frac{\partial \underline{E}}{\partial p} \right) \frac{dp}{g} \quad (6)$$

(6) shows that the structure of the convective fluxes is closely linked to the structure of the specified reference profile \underline{E} . By adjusting toward an observationally realistic thermodynamic structure \underline{E} , the convective fluxes including precipitation are simultaneously constrained to have a structure similar to those derived diagnostically from (1) (or its simplified form (6)) by the budget method (Yanai et al., 1973; Nitta, 1977).

Adjustment Procedure

The large-scale advective terms, radiation, and surface fluxes are allowed to modify the thermodynamic structure \underline{S} . Cloudtop is then found using a moist adiabat through the surface θ_E . Cloudtop height distinguishes shallow from deep convection (currently level 11 in the grid point model; about 760 mb). Different reference profiles are constructed for shallow and deep convection that satisfy different energy integral constraints. The convective adjustment, $(\underline{E} - \underline{S})/\tau$, is then applied. This implicitly redistributes heat and moisture in the atmosphere as it is adjusted toward \underline{E} .

The deep convection reference profile \underline{E}_D is constructed to satisfy the total enthalpy constraint.

$$\int_{p_0}^{p_T} (H_E - H_S) dp = 0_D \quad (7)$$

where $H = C_p T + Lq$ and p_0 , p_T are a surface (or low level) and cloudtop pressure, respectively. The precipitation rate is then given by

$$P = \int_{p_0}^{p_T} \left(\frac{q_E - \bar{q}}{\tau} \right) \frac{dp}{g} = - \frac{C_p}{L} \int_{p_0}^{p_T} \left(\frac{T_E - \bar{T}}{\tau} \right) \frac{dp}{g} \quad (8)$$

No liquid water is stored in the present scheme. The adjustment is suppressed if it ever gives $P < 0$.

For shallow convection, the reference profile \underline{E}_S is constructed to satisfy the two separate energy constraints

$$\int_{P_0}^{P_T} C_p (T_E - \bar{T}) dp = \int_{P_0}^{P_T} L(q_E - \bar{q}) dp = 0 \quad (9)$$

so that the integrated condensation (and precipitation) rates are zero.

Reference Thermodynamic Profiles

The essence of this convective adjustment scheme is these reference profiles. Shallow and deep convection are separated by cloudtop.

SINGLE COLUMN TESTS USING GATE-WAVE, BOMEX, ATEX AND ARCTIC AIRMASS DATA SETS

The convective parameterization scheme was tested and tuned using a series of single column data sets. A GATE-wave data set (derived from Thompson et al., 1979) was used to test and develop the deep convection scheme. BOMEX (from Holland and Rasmusson, 1973) and ATEX (from Augstein et al., 1973; Wagner, 1975) data sets were used to test and develop the shallow convection scheme. A fourth data set for an Arctic air-mass transformation (from Okland, 1976) was used to test both schemes with strong surface fluxes. Only the first part of the GATE tests is shown in this abbreviated paper.

Deep Convection

GATE-Wave Data Set

The grid point model is run as a single column model with prescribed GATE Phase III radiation (from Cox and Griffith, 1979) and prescribed heat and moisture tendencies due to adiabatic processes (from Thompson et al., 1979). The adiabatic forcing terms have a wave structure with an 80-hour period. The model is integrated in time using the convection scheme from an initial sounding. The temperature and moisture structure, the precipitation, and the vertical profile of the convective heating and drying terms as a function of time can be compared with those diagnosed from observations. Most of the sensitivity tests will be done with prescribed surface fluxes (from Thompson et al., 1979), using an 18-level model. A section follows showing results with an interactive boundary layer scheme.

Optimum Parameter Set

First, an optimum parameter set is presented to show how well the scheme can reproduce the structure of the mean GATE-wave (Table 1). The model scheme decreases linearly from -25 at the surface to -50 at the freezing level and returns to -38 at cloudtop.

TABLE 1 Convection Scheme Parameters

| τ | O | F | τ | α |
|--------|-----|-----|--------|----------|
| 2 hr | -25 | -50 | -38 | 1.5 |

Figure 4 shows the 80-hour mean vertical structure of the prescribed adiabatic forcing terms and the model physics (convective scheme plus prescribed radiation and surface fluxes). The mean balance is very precise, although the lower troposphere cools and the upper troposphere warms slightly. Figures 5a and 5b show the computed 40- and 80-hour soundings compared with the observations showing the same result. At 40 hours (the wave trough) the agreement between model scheme and the observed mean structure is very good, although the convection scheme does not reproduce the subsequent drying out of the upper troposphere at the ridge (80 hours). Figures 6, 7, and 8 compare the time-height cross-sections for the data (observed structure and diagnosed convective source terms) with these predicted by the model using the convection scheme.

Figure 6 shows the wave in equivalent potential temperature for the data and structure produced using the convection scheme. The agreement is good, although as in Figure 5, the data is warmer and moister at the lowest level. Figure 7 shows the same comparison for relative humidity showing fairly good agreement. The convection scheme does not maintain relative humidity well at 200 mb near cloudtop. Figures 8 and 9 compare diagnosed and computed convective heat source and moisture sink (plus surface fluxes), showing how well the parameterization scheme reproduces the general wave structure of the convective source terms with their maximum at different pressure levels. The agreement is excellent.

Figure 10 compares the observed rainfall and that computed by the model. Good agreement is seen in amplitude but not in phase. The convection scheme, which is closely coupled to the moisture advection, cannot reproduce the observed lag of the precipitation that appears to be due to subgrid-scale storage of moisture, presumably in the cloudfields (Betts, 1978; Frank, 1978).

In general, the parameterization scheme does well in reproducing the structure of the convective source terms and the precipitation. In its present form, it does not reproduce subgrid-scale moisture storage. The deficiencies in the low-level structure seen in Figure 5 can be markedly reduced using an improved resolution and an interactive surface boundary layer. Some deficiencies near cloudtop are always

715

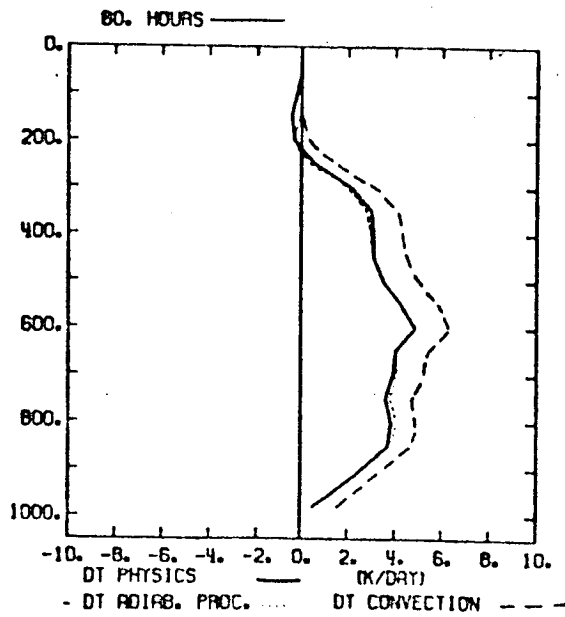
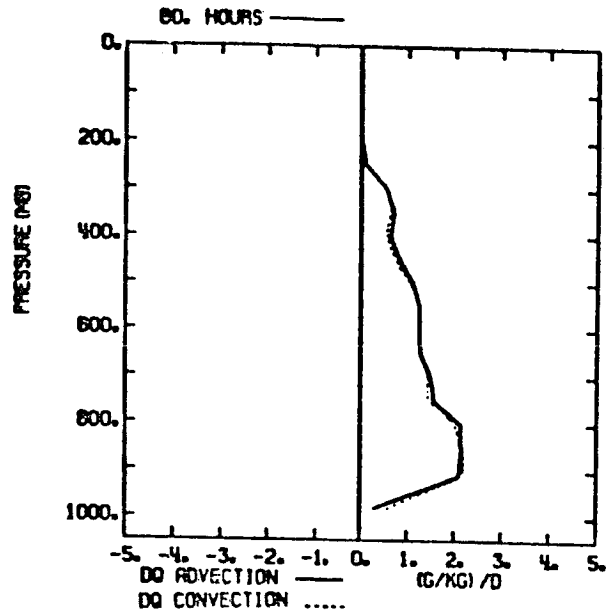


FIGURE 4 Eighty hours mean vertical structure of prescribed adiabatic forcing terms and parameterized convective drying and heating for GATE-wave.

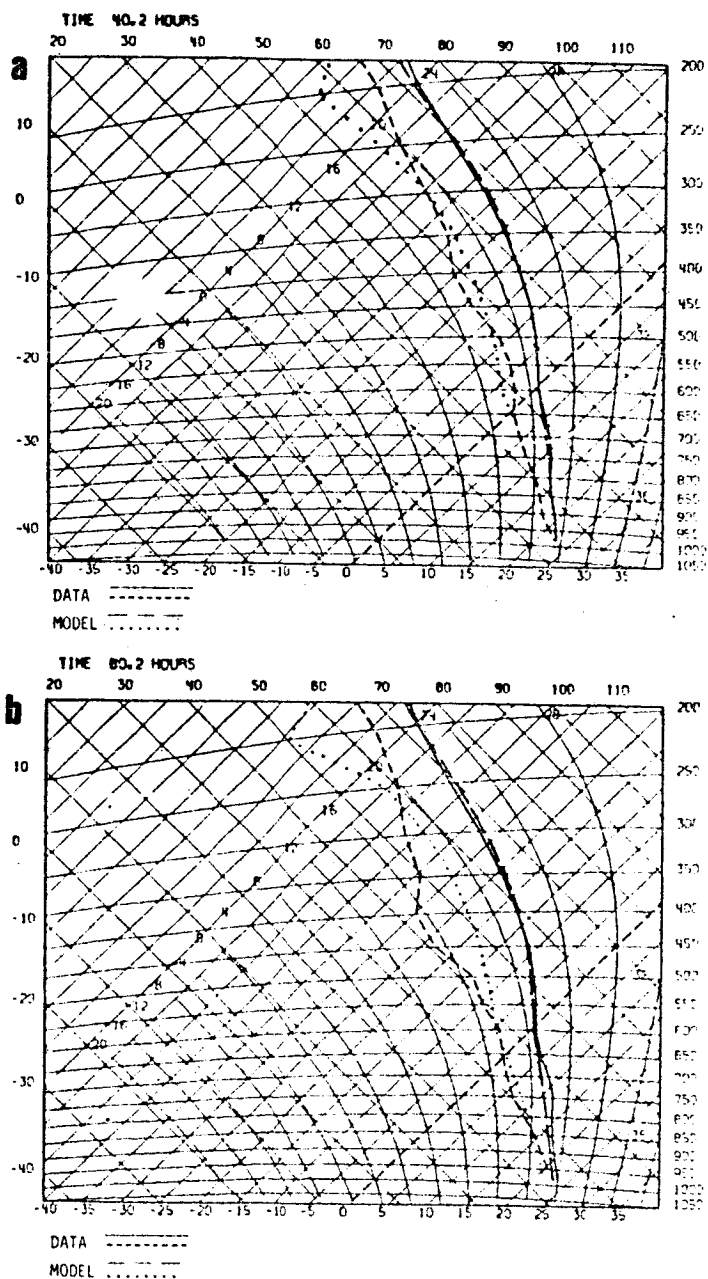


FIGURE 5 (a) Comparison at 40 hours (trough) of observed sounding (T , T_D solid and dashed) and computed sounding (long dash and dots).
 (b) Comparison at 80 hours (ridge) of observed sounding (T , T_D solid and dashed) and computed sounding (long dash and dots).

717

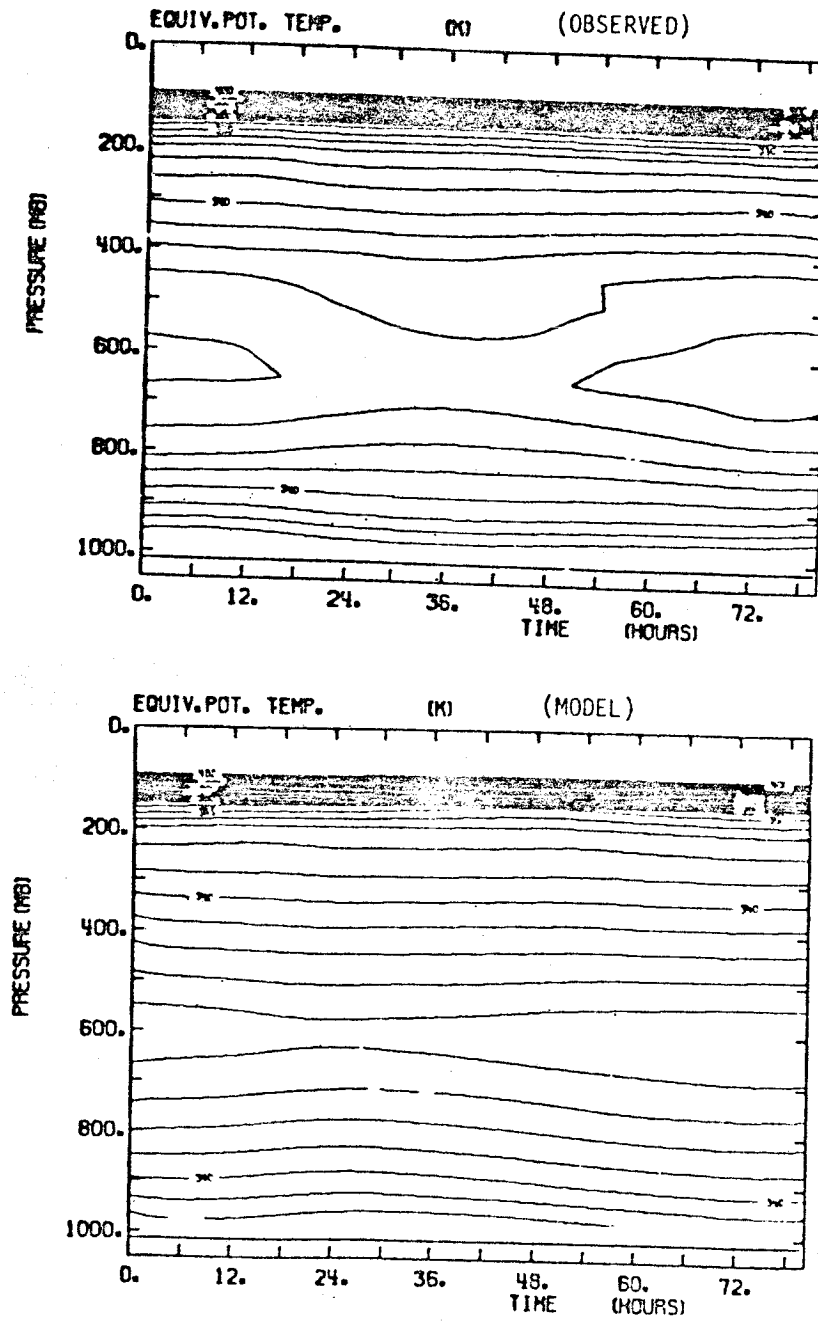


FIGURE 6 Comparison of observed (above) and computed (below) θ_E structure of GATE-wave data.

718

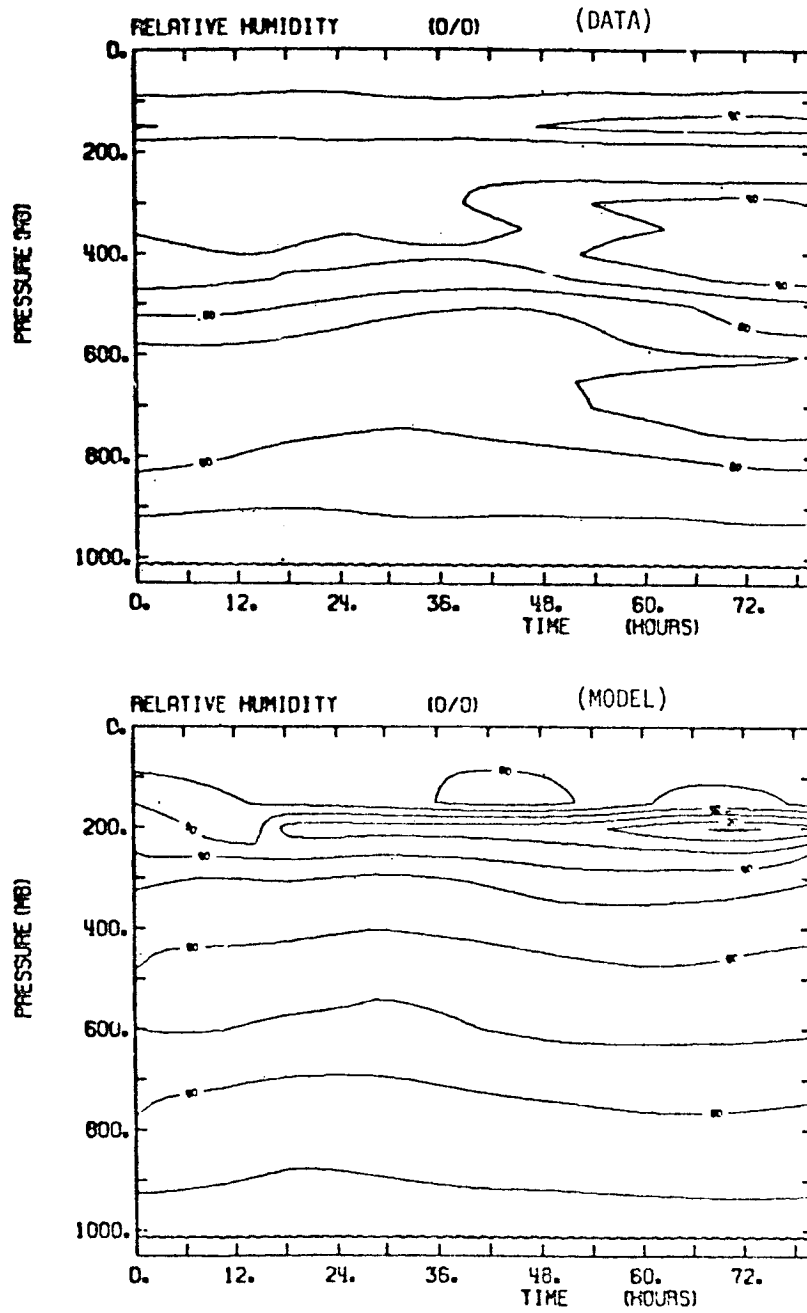


FIGURE 7 Comparison of observed (above) and computed (below) relative humidity for GATE-wave data.

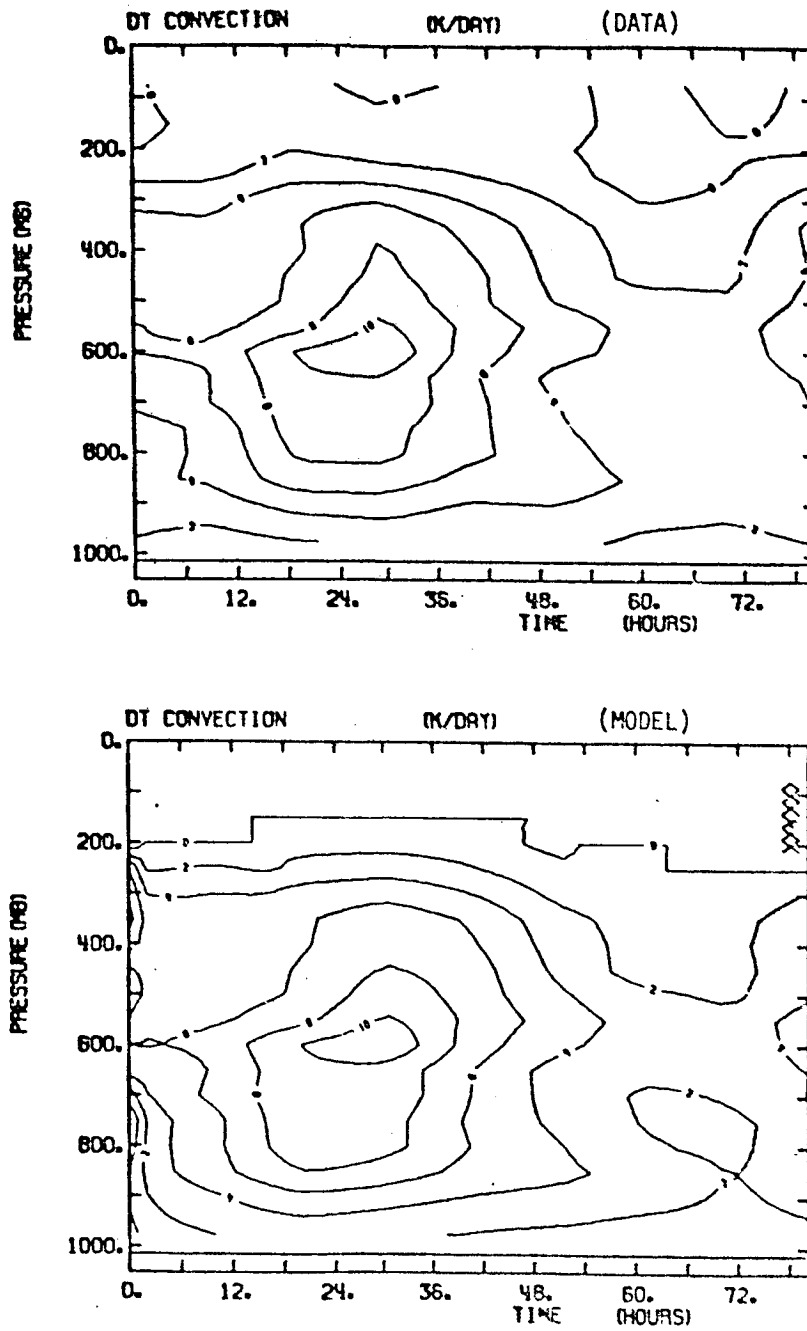


FIGURE 8 Comparison of diagnosed and computed convective heating for GATE-wave data.

720

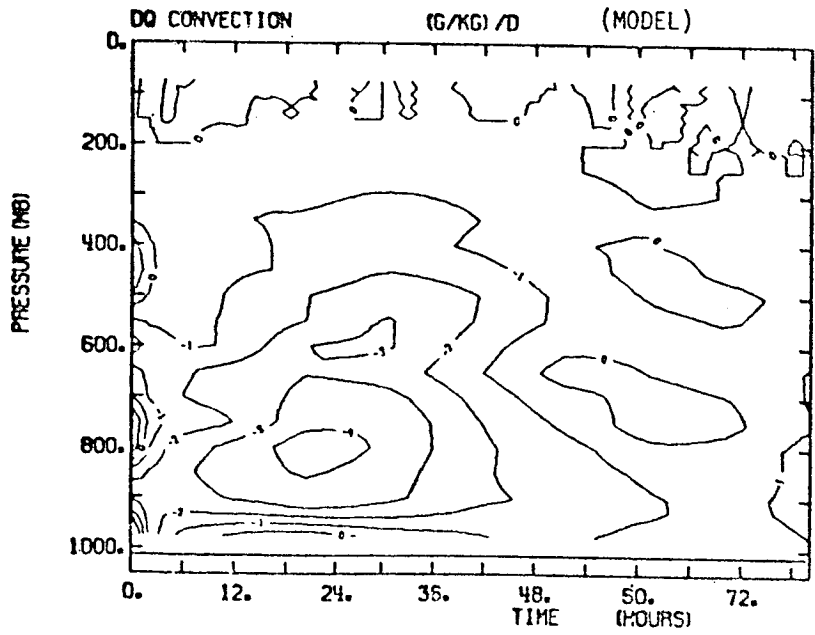
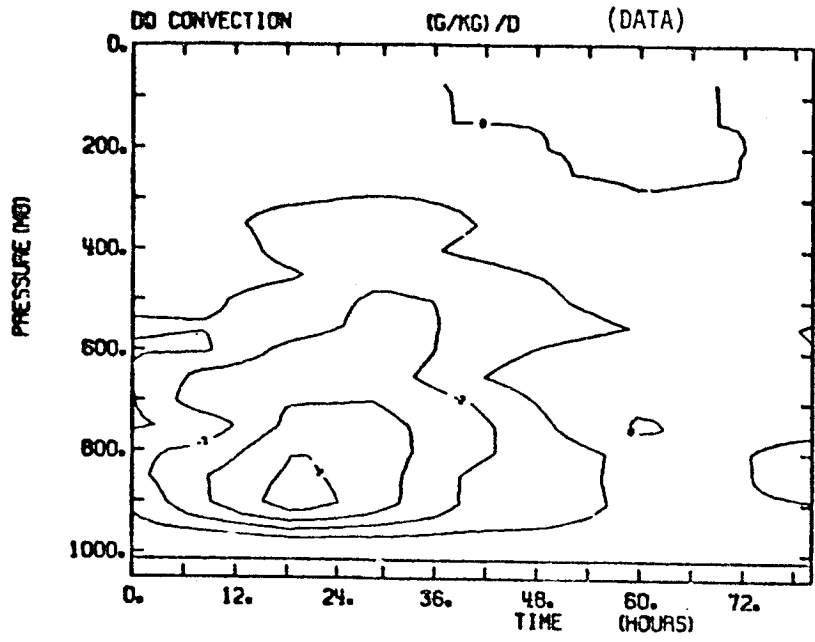


FIGURE 9 Comparison of diagnosed and computed convective drying for GATE-wave data.

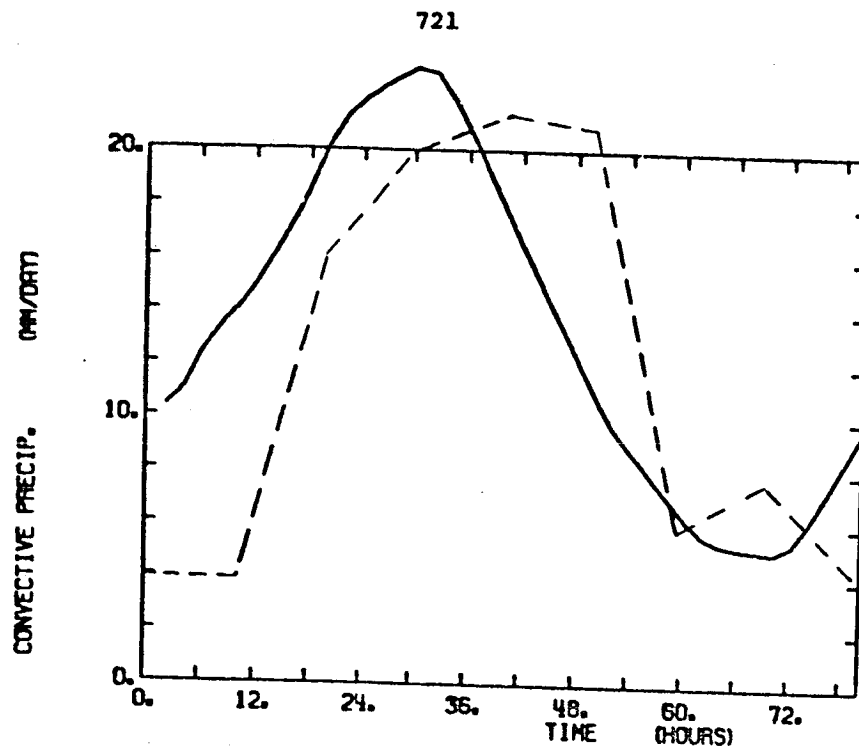


FIGURE 10 Comparison of observed (dashed) and computed rainfall.

likely because the adjustments at this level are always sensitive to the exact specification of cloudtop height in terms of the limited model vertical resolution. Further tuning may be possible. The GATE tests were first run with a cloudtop interpolated between model levels in the specification of the adjustment profile. However this proved to be an unnecessary complication and was dropped from the scheme for the subsequent interactive boundary layer test and global model tests. In this section, the interpolated cloudtop has been retained because a few of the results, although substantially the same, are smoother (cloudtop does not jump between levels) and are therefore easier to intercompare.

ACKNOWLEDGMENTS

Supported by the European Centre for Medium Range Weather Forecasts and the National Science Foundation under Grant ATM-8120444.

REFERENCES

- Arakawa, A., and W.H. Schubert (1974). Interaction of a cumulus cloud ensemble with the large-scale environment: Part I. J. Atmos. Sci. 31, 674-701.

- Albrecht, B.A., A.K. Betts, W.H. Schubert, and S.K. Cox (1979). A model of the thermodynamic structure of the trade-wind boundary layer: Part II. Theoretical formulation and sensitivity tests. J. Atmos. Sci. 36, 73-89.
- Augstein, E., H. Riehl, F. Ostopoff, and V. Wagner (1973). Mass and energy transports in an undisturbed Atlantic trade-wind flow. Mon. Wea. Rev. 101, 101-111.
- Barnes, G.M., and K. Sieckman (1984). The environment of fast and slow tropical mesoscale convective cloud lines. Mon. Wea. Rev. 112, 1782-1794.
- Betts, A.K. (1973). Non-precipitating cumulus convection and its parameterization. Quart. J. Roy. Meteorol. Soc. 99, 178-196.
- Betts, A.K. (1974). The scientific basis and objectives of the U.S. Convection Subprogram for the GATE. Bull. Amer. Meteorol. Soc. 55, 304-313.
- Betts, A.K. (1978). Convection in the tropics. Meteorology over the tropical oceans, D.B. Shaw, Roy. Meteorol. Soc., 105-132.
- Betts, A.K. (1982a). Saturation point analysis of moist convective overturning. J. Atmos. Sci. 39, 1484-1505.
- Betts, A.K. (1982b). Cloud thermodynamic models in saturation point coordinates. J. Atmos. Sci. 39, 2182-2191.
- Betts, A.K. (1983). Thermodynamics of mixed stratocumulus layers: Saturation point budgets. J. Atmos. Sci. 40, 2655-2670.
- Betts, A.K., and M.J. Miller (1984). A new convective adjustment scheme. Tech. Rpt. No. 43, ECMWF, Reading RG2 9AX, England, 68 pp.
- Cox, S.K., and K.T. Griffith (1979). Estimates of radiative flux divergence during Phase III of the GARP Atlantic Tropical Experiment, Part II: Analysis of Phase III results. J. Atmos. Sci. 36, 586-601.
- Frank, W.M. (1977). The structure and energetics of the tropical cyclone, Part I: Storm structure. Mon. Wea. Rev. 105, 1119-1135.
- Frank, W.M. (1978). The life cycles of GATE convective systems. J. Atmos. Sci. 35, 1256-1261.
- Frank, W.M. (1983). The cumulus parameterization problem. Mon. Wea. Rev. 111, 1859-1871.
- Holland, J.Z., and E.M. Rasmusson (1973). Measurements of the atmospheric mass, energy and momentum budgets over a 500 km square of tropical ocean. Mon. Wea. Rev. 101, 44-55.
- Houze, R.A., and A.K. Betts (1981). Convection in GATE. Rev. Geophys. Space Phys. 19, 541-576.
- Kuo, H.L. (1965). On formation and intensification of tropical cyclones through latent heat release by cumulus convection. J. Atmos. Sci. 22, 40-63.
- Kuo, H.L. (1974). Further studies of the parameterization of the influence of cumulus convection of large-scale flow. J. Atmos. Sci. 31, 1232-1240.
- Lord, S.J. (1982). Interaction of a cumulus cloud ensemble with the large-scale environment. Part III: Semi-prognostic test of the Arakawa-Schubert cumulus parameterization. J. Atmos. Sci. 39, 88-103.

- Manabe, S., J. Smagorinsky, and R.F. Strickler (1965). Simulated climatology of a general circulation model with a hydrologic cycle. Mon. Wea. Rev. 93, 769-798.
- Nitta, T. (1977). Response of cumulus updraft and downdraft to GATE A/B-scale motion systems. J. Atmos. Sci. 34, 1163-1186.
- Ooyama, K. (1971). A theory of parameterization of cumulus convection. J. Meteorol. Soc. Japan 49, 744-756.
- Okland, H. (1976). An example of air-mass transformation in the Arctic and convective disturbances of the windfield. Report DM-20, Univ. of Stockholm, 30 pp.
- Thompson, Jr., R.M., S.W. Payne, E.E. Reckel, and R.J. Reed (1979). Structure and properties of synoptic-scale wave disturbances in the intertropical convergence zone of the eastern Atlantic. J. Atmos. Sci. 36, 53-72.
- Wagner, V. (1975). Relationships between the tropospheric circulation and energetic processes within the Hadley circulation over the Atlantic Ocean. Berichte Inst. Radiometeor. und Maritime Meteor., Univ. Hamburg, No. 26, 83 pp.
- Yanai, M., S. Esbensen, and J.H. Chu (1973). Determination of bulk properties of tropical cloud clusters from large-scale heat and moisture budgets. J. Atmos. Sci. 30, 611-627.